Structural and Thermal Studies on Salicylato Complexes of Divalent Manganese, Nickel, Copper and Zinc

Kari Rissanen,[a] Jussi Valkonen,[a] Pertti Kokkonen[b] and Markku Leskelä[b,*]

[a]Department of Chemistry, University of Jyväskylä, SF-40100 Jyväskylä and [b]Department of Chemistry, University of Oulu, SF-90570 Oulu, Finland

Rissanen, K., Valkonen, J., Kokkonen, P. and Leskelä, M., 1987. Structural and Thermal Studies on Salicylato Complexes of Divalent Manganese, Nickel, Copper and Zinc. – Acta Chem. Scand., Ser. A 41: 299–309.

The crystal structures of $[Mn(Hsal)_2(H_2O)_2]_2$ (**1**) and $[Ni(Hsal)_2(H_2O)_4]$ (**2**) were solved and those of $[Cu(Hsal)_2(H_2O)_2]\cdot 2H_2O$ (**3**), and $[Zn(Hsal)_2(H_2O)_2]$ (**4**) were redetermined from X-ray diffractometer data [Hsal = $C_6H_4(OH)COO^-$]. The complexes **1–3** belong to the monoclinic space group $P2_1/c$ but are not isomorphic. The space group of **4** is $C2$. The coordination of the M^{2+} ion is different in each complex: Mn^{2+} has pentagonal bipyramidal, Ni^{2+} octahedral and Cu^{2+} square-planar coordination, while Zn^{2+} has, irregularly, six oxygen atoms in the coordination kernel with four short (2.0 Å) and two long (2.5 Å) Zn–O distances. Complex **1** is dinuclear with symmetry-related Mn atoms at a mutual distance of 3.7 Å. The geometry of the salicylato ligands in each complex is quite normal.

The thermal behaviour of the complexes has been studied by TG and high resolution mass spectrometric methods. After dehydration the salicylato ligands are released in two stages and they decompose further to smaller molecules. The fragmentation pattern of the salicylato ligands is different in the two stages.

The solid salicylato (2-hydroxybenzoato) complexes of transition metals are structurally and thermally poorly characterized in the literature. There are two previous structure determinations involving copper complexes: $[Cu(Hsal)_2(H_2O)_2]\cdot 2H_2O$[1] and $[Cu(Hsal)_2(H_2O)_2]$[2] [Hsal = $C_6H_4(OH)COO^-$]. Two other salicylato structures reported in the literature are those of $[Zn(Hsal)_2(H_2O)_2]$ and $[Co(Hsal)_2(H_2O)_4]$.[3,4] For the manganese salicylato complex only the unit cell and space group have been reported.[5]

Reports of thermoanalytical studies of salicylato complexes are sparse. Studies on VO^{2+}, Fe^{2+}, Co^{2+}, Cu^{2+} and Zn^{2+} complexes have been described in the literature but they are somewhat contradictory.[6–9] Some substituted (particularly halogen-substituted) complexes have also been investigated.[10]

In the present paper we report the crystal structures, thermal behaviour and IR spectra of $[Mn(Hsal)_2(H_2O)_2]_2$ (**1**), $[Ni(Hsal)_2(H_2O)_4]$ (**2**), $[Cu(Hsal)_2(H_2O)_2]\cdot 2H_2O$ (**3**) and $[Zn(Hsal)_2(H_2O)_2]$ (**4**). The thermal behaviour of $[Co(Hsal)_2(H_2O)_4]$ and $[Cu(Hsal)_2(H_2O)_2]$ has also been studied for comparison.

Experimental

Syntheses. The salicylato complexes were crystallized at room temperature from aqueous solutions of salicylic acid and the metal sulfates adjusted to pH ca. 5.5 with NaOH. In the case of Co^{2+}, Ni^{2+} and Zn^{2+}, salicylic acid was used in excess (H_2sal/MSO_4 = 1:0.33), while for Mn^{2+} and Cu^{2+} the ratio was about 1:1. The concentration of salicylic acid ranged between 0.5 and 1 mol dm^{-3} and that of metal salt between 0.2 and 0.5 mol dm^{-3}. Crystals large enough for X-ray diffraction studies were grown in 1–4 days. All crystals formed were of bis(salicylato) complexes. The synthesis of $[Cu(Hsal)_2(H_2O)_2]$ was carried out according to Jagner *et al.*[2]

*Present address: Department of Chemistry and Biochemistry, University of Turku, SF-20500 Turku, Finland.

Table 1. Conditions for unit cell determination and data collection.

Formula	$[Mn(Hsal)_2(H_2O)_2]_2$	$[Ni(Hsal)_2(H_2O)_4]$	$[Cu(Hsal)_2(H_2O)_2]\cdot 2H_2O$	$[Zn(Hsal)_2(H_2O)_2]$
Formula weight	730.36	404.96	409.81	375.62
a/Å	15.605(11)	6.781(5)	3.741(2)	15.450(18)
b/Å	12.298(10)	5.163(3)	17.667(16)	5.341(3)
c/Å	7.629(1)	24.177(14)	12.278(14)	9.164(5)
β/°	96.66(4)	107.14(5)	93.37(7)	93.55(7)
V/Å^3	1454.2(16)	808.9(9)	810.1(13)	754.8(10)
Space group	$P2_1/c$ (No. 14)	$P2_1/c$ (No. 14)	$P2_1/c$ (No. 14)	$C2$ (No. 5)
d_{calc}/g cm^{-3}	1.67	1.66	1.68	1.65
Z	2	2	2	2
μ/cm^{-1}	9.11	12.54	13.40	17.02
F(000)	748	420	422	384
Crystal size/mm	0.2×0.2×0.3	0.15×0.20×0.15	0.20×0.25×0.15	0.2×0.25×0.25
Temperature/°C	23±1	23±1	23±1	23±1
Radiation	Mo*K*α	Mo*K*α	Mo*K*α	Mo*K*α
No. of refl. used in unit cell detmn.	15	15	15	12
Range of refl. used in unit cell detmn. /2θ	6.61–22.39	3.54–25.65	4.05–13.19	4.44–11.89
Data collection method	θ/2θ	θ/2θ	θ/2θ	θ/2θ
Scan speed/°min^{-1}	6.0	2.0	2.0	2.0
Range of data collection/2θ	5–60	5–60	5–50	5–60
Number of collected reflections	4434	2793	1742	2491
No. of refl. used in refinement [$I>3\sigma(I)$]	2871	1643	930	708
R(iso)	0.076	0.073	0.112	0.109
R(aniso)[a]	0.034	0.029	0.035	0.042
R_w (aniso)[a]($w=1$)	0.036	0.033	0.039	0.048

[a]Non-hydrogen atoms with anisotropic and hydrogen atoms with fixed isotropic temperature factors.

X-ray diffraction. The structures of the complexes were determined from single-crystal X-ray diffraction data collected on a Syntex $P2_1$ diffractometer. The crystal data as well as the details of the structure determinations are given in Table 1. One reference reflection was used to monitor the stability of each crystal. The intensities of these standard reflections were remeasured after every 99 reflections; no decrease in their intensities was observed. The intensities of the reflections were corrected for Lorentz and polarization effects but no absorption correction was needed.

The position of Mn in **1** was located using direct methods. The subsequent electron density calculations gave the positions of the other atoms. The structure of **2** turned out to be isomorphous with the corresponding cobalt complex and the atomic coordinates were obtained from that structure.[4] The structures of **3** and **4** are redetermined in the present work, and the atomic positions for the refinements have been taken from the previous structure reports.[1,3] Block-diagonal refinements based on structure factors and unit weights were used. The scattering factors were those of Cromer and Mann given for neutral atoms.[11] In final calculations, non-hydrogen atoms had anisotropic temperature factors while the hydrogen atoms had fixed isotropic temperature factors. In the calculations the following crystallographic program packages were used: MITHRIL,[12] XRAY 76[13] and ORTEP.[14]

A list of the anisotropic temperature factors as well as the observed and calculated structure factors is obtainable from the author (J.V.) upon request.

Thermal analyses. The thermoanalytical measurements were carried out with a Mettler TA 3000 thermoanalyzer. Sample weights of 5–10 mg and a heating rate of 5 °C min^{-1} were used. A nitrogen atmosphere (continuous flow) was used in most experiments. The mass spectra of the decomposition products were recorded with a Kratos MS 80 RF high resolution mass spectrometer. The experimental technique has been described elsewhere.[15]

Infrared spectra. The IR spectra were recorded on a Perkin-Elmer 457 instrument using the KBr pellet technique. The absorption frequencies observed were as follows (cm^{-1}): **1**: 3490 s, 3420 s, 3170 s, 3080 s, 2760 vw, 1630 vs, 1600 vs, 1570 sh, 1555 sh, 1540 vs, 1485 vs, 1470 vs, 1400 vs, 1350 vs, 1310 s, 1250 vs, 1245 sh, 1150 s, 1140 s, 1090 w, 1030 m, 965 vw, 950 vw, 880 s, 865 sh, 810 s, 760 sh, 740 vs, 690 s, 665 s, 565 w, 530 m, 460 w, 385 m. **2**: 3490 s, 3415 s, 3250 s, 2960 vw, 2930 vw, 2870 vw, 2770 vw, 2700 vw, 2600 vw, 2510 vw, 1960 vw, 1925 vw, 1630 s, 1590 vs, 1570 vs, 1510 sh, 1485 vs, 1460 vs, 1410 sh, 1395 vs, 1335 vs, 1305 m, 1245 vs, 1160 sh, 1145 vs, 1125 sh, 1030 m, 995 vw, 985 vw, 885 vw, 860 m, 820 w, 755 vs, 695 s, 675 s, 635 sh, 615 w, 575 w, 530 w, 400 m. **3**: 3560 s, 3410 vs, 2930 s (broad), 2450 w, 1630 vs, 1595 vs, 1565 sh, 1550 vs, 1490 vs, 1450 vs, 1415 sh, 1400 vs, 1360 vs, 1310 m, 1255 vs, 1150 m, 1100 vw, 1035 w, 890 vw, 860 m, 815 m, 770 sh, 740 s, 690 m, 665 m, 565 w, 530 m, 450 m. **4**: 3310 s, 3110 s, 2480 w, 1975 w, 1945 vw, 1925 vw, 1870 vw, 1835 w, 1625 vs, 1600 vs, 1585 sh, 1530 sh, 1485 vs, 1470 vs, 1385 vs, 1340 vs, 1315 sh, 1240 vs, 1200 sh, 1150 s, 1095 w, 1035 m, 995 vw, 965 w, 875 s, 815 m, 805 sh, 790 sh, 760 vs, 700 s, 670 s, 570 m, 530 m, 505 w, 400 m (vs = very strong, s = strong, m = medium, w = weak, vw = very weak and sh = shoulder).

Results

Crystal structures. Fractional coordinates for all compounds are listed in Tables 2–5, and bond distances in Tables 6 and 7.

The geometry of the salicylato ligands is similar in all four complexes, and the metal atom appears to have no appreciable influence on the conformation of these ligands. The C–C bonds in the benzene ring are normal: The average C–C distances are 1.39, 1.39, 1.38 and 1.38 Å for **1–4**, respectively, and the length of the C–C single bond between the benzene ring and the carboxyl group varies from 1.474 to 1.513 Å. The C–O distances in the carboxyl group are almost equal, only the bond involving the coordinated oxygen atom being slightly lengthened as would be expected. In this respect the Cu^{2+} complex is an exception because both the C-O distances are about 1.26 Å.

Least-squares refinement revealed that the salicylato ligands are planar in **1**, **2** and **4**. In the copper complex the carboxyl groups are twisted away from the plane of the benzene ring (Fig. 3). Similar twisting has been observed in $[Cu(Hsal)_2(H_2O)_2]$.[2] The phenol OH groups are oriented

Table 2. Fractional coordinates and temperature factors, U_{eq} for $[Mn(Hsal)_2(H_2O)_2]_2$ [$U_{eq} = {}^1/_3 \cdot 100 \cdot (U_{11}+U_{22}+U_{33})$].

Atom	*x*	*y*	*z*	U_{eq}
Mn	0.58745(1)	0.10287(1)	0.50724(1)	2.34
O(1)	0.73059(3)	0.09846(5)	0.58098(8)	4.58
O(2)	0.67437(3)	0.26029(4)	0.54434(7)	3.87
O(3)	0.88633(4)	0.07072(5)	0.72325(10)	6.36
O(4)	0.59701(4)	0.08724(4)	0.22937(6)	4.20
O(5)	0.57474(3)	0.09604(4)	0.79029(6)	4.02
O(11)	0.48474(3)	0.22744(4)	0.48049(7)	3.50
O(12)	0.42450(3)	0.06904(4)	0.48965(8)	4.18
O(13)	0.40047(3)	0.40214(4)	0.50575(7)	4.13
C(1)	0.82222(4)	0.24726(6)	0.66761(9)	3.29
C(2)	0.89119(5)	0.17981(7)	0.73024(10)	4.24
C(3)	0.96775(5)	0.22670(9)	0.80581(13)	5.95
C(4)	0.97682(6)	0.33515(10)	0.81561(13)	6.65
C(5)	0.91013(7)	0.40435(9)	0.75224(14)	6.71
C(6)	0.83331(6)	0.35867(7)	0.67949(12)	4.95
C(7)	0.73887(4)	0.20079(6)	0.59235(9)	3.21
C(11)	0.33832(4)	0.22463(5)	0.53361(8)	2.63
C(12)	0.33282(4)	0.33718(5)	0.53768(9)	3.03
C(13)	0.25774(5)	0.38815(7)	0.57651(10)	4.27
C(14)	0.18825(5)	0.32525(8)	0.60998(11)	4.97
C(15)	0.19259(5)	0.21402(8)	0.60628(12)	4.88
C(16)	0.26721(5)	0.16357(6)	0.56784(10)	3.83
C(17)	0.41919(4)	0.16994(5)	0.49785(8)	2.67
H(1)	0.0038(5)	0.3125(7)	0.3470(11)	5.00
H(2)	0.0277(5)	0.3884(7)	0.8697(11)	5.00
H(3)	0.0881(5)	0.5135(7)	0.2361(11)	5.00
H(4)	0.2103(5)	0.5921(7)	0.3692(10)	5.00
H(5)	0.1524(5)	0.9541(7)	0.3132(11)	5.00
H(6)	0.3937(5)	0.5189(7)	0.3166(11)	5.00
H(7)	0.3718(5)	0.6437(7)	0.3240(11)	5.00
H(8)	0.4175(5)	0.9741(7)	0.1551(11)	5.00
H(9)	0.4001(5)	0.8454(7)	0.1531(11)	5.00
H(11)	0.2578(5)	0.4750(7)	0.5780(11)	5.00
H(12)	0.1384(5)	0.3587(7)	0.6487(11)	5.00
H(13)	0.1423(5)	0.1753(7)	0.6433(11)	5.00
H(14)	0.2760(5)	0.0811(7)	0.5648(11)	5.00
H(15)	0.4454(5)	0.3440(7)	0.4935(11)	5.00

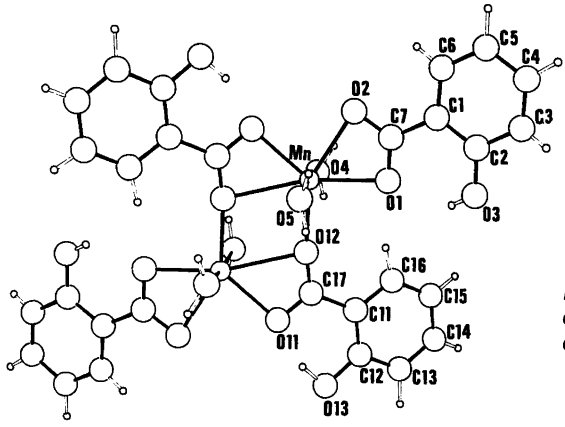

Fig. 1. A perspective view of the molecular structure of $[Mn(Hsal)_2(H_2O)_2]_2$ (**1**) showing also the numbering of the atoms.

Table 3. Fractional coordinates and temperature factors, U_{eq}, for $[Ni(Hsal)_2(H_2O)_4]$.

Atom	*x*	*y*	*z*	U_{eq}/Å^2
Ni	1.00000(0)	0.50000(0)	0.50000(0)	2.10
O(1)	0.79826(8)	0.34842(12)	0.42887(3)	3.01
O(2)	0.49219(8)	0.48570(15)	0.43296(3)	3.69
O(3)	0.83700(8)	−0.01357(14)	0.36514(2)	3.44
O(4)	0.85976(8)	0.29580(12)	0.55347(3)	3.04
O(5)	0.79803(9)	0.79945(12)	0.49599(3)	3.63
C(1)	0.50497(11)	0.14096(16)	0.36821(3)	2.42
C(2)	0.62763(11)	−0.02910(17)	0.34709(3)	2.63
C(3)	0.53791(13)	−0.21838(18)	0.30656(4)	3.47
C(4)	0.32612(14)	−0.23717(20)	0.28649(4)	3.82
C(5)	0.20170(13)	−0.07140(21)	0.30658(4)	3.96
C(6)	0.29005(12)	0.11649(19)	0.34707(4)	3.34
C(7)	0.59858(11)	0.34090(16)	0.41263(3)	2.51
H(1)	0.3738(16)	0.1538(22)	0.2059(4)	5.00
H(2)	0.2594(15)	0.8686(21)	0.7602(4)	5.00
H(3)	0.0524(15)	0.5937(21)	0.7924(4)	5.00
H(4)	0.2080(15)	0.2544(22)	0.3629(4)	5.00
H(5)	0.1338(16)	0.6297(21)	0.1110(4)	5.00
H(6)	0.0567(15)	0.7606(22)	0.9159(4)	5.00
H(7)	0.2244(15)	0.6257(21)	0.4354(4)	5.00
H(8)	0.3097(15)	0.2270(22)	0.5188(4)	5.00
H(9)	0.2008(15)	0.0497(21)	0.4862(4)	5.00

Table 4. Fractional coordinates and temperature factors, U_{eq}, for $[Cu(Hsal)_2(H_2O_2] \cdot 2H_2O$.

Atom	*x*	*y*	*z*	U_{eq}/Å^2
Cu	0.00000(0)	0.50000(0)	0.50000(0)	3.66
O(1)	0.24889(32)	0.35907(6)	0.38882(8)	4.84
O(2)	−0.03289(31)	0.46711(6)	0.34921(8)	4.19
O(3)	0.22239(37)	0.25130(7)	0.25452(10)	5.96
O(4)	−0.33239(41)	0.42384(8)	0.53961(10)	7.30
O(5)	0.44694(41)	0.39782(8)	0.73476(10)	7.11
C(1)	−0.00099(39)	0.37548(8)	0.20956(11)	3.25
C(2)	0.07647(43)	0.30136(9)	0.18056(12)	3.88
C(3)	0.00270(47)	0.27612(10)	0.07505(14)	4.76
C(4)	−0.14105(48)	0.32518(11)	−0.00196(13)	5.33
C(5)	−0.21724(48)	0.39894(11)	0.02377(13)	4.97
C(6)	−0.14826(45)	0.42384(9)	0.12977(12)	4.12
C(7)	0.07502(42)	0.40237(9)	0.32315(12)	3.59
H(1)	0.0801(40)	0.2254(9)	0.0603(12)	5.00
H(2)	−0.1385(39)	0.3128(9)	−0.0757(12)	5.00
H(3)	−0.2971(39)	0.4375(9)	−0.0256(12)	5.00
H(4)	−0.1865(39)	0.4849(8)	0.1558(12)	5.00
H(5)	0.1998(41)	0.2767(9)	0.3243(12)	5.00
H(6)	0.4287(40)	0.9184(9)	0.9226(12)	5.00
H(7)	0.3029(40)	0.6041(9)	0.4914(12)	5.00
H(8)	0.3366(39)	0.8815(9)	0.7666(12)	5.00
H(9)	0.2011(39)	0.0942(9)	0.2409(12)	5.00

Table 5. Fractional coordinates and temperature factors, U_{eq}, for $[Zn(Hsal)_2(H_2O)_2]$.

Atom	*x*	*y*	*z*	U_{eq}/Å^2
Zn(1)	1.0000(0)	0.0000(0)	0.0000(0)	3.62
O(1)	0.8990(2)	0.1522(8)	0.0896(4)	4.52
O(2)	1.0139(2)	0.3232(8)	0.2009(5)	5.15
O(3)	0.7488(2)	0.3431(9)	0.1109(5)	5.37
O(4)	1.0767(2)	−0.2442(8)	0.1111(5)	6.17
C(1)	0.8757(2)	0.5033(21)	0.2484(4)	3.37
C(2)	0.7867(3)	0.5006(20)	0.2089(5)	3.53
C(3)	0.7354(3)	0.6807(12)	0.2717(6)	4.41
C(4)	0.7705(4)	0.8488(13)	0.3684(7)	5.49
C(5)	0.8595(4)	0.8441(13)	0.4127(7)	5.56
C(6)	0.9094(3)	0.6662(13)	0.3495(6)	4.46
C(7)	0.9332(3)	0.3163(10)	0.1768(6)	3.73
H(1)	0.320(3)	0.675(12)	0.762(5)	5.00
H(2)	0.237(3)	0.458(11)	0.412(5)	5.00
H(3)	0.390(3)	0.434(9)	0.480(5)	5.00
H(4)	0.474(3)	0.156(11)	0.373(5)	5.00
H(5)	0.234(3)	0.267(11)	0.907(5)	5.00
H(6)	0.442(3)	0.100(10)	0.850(5)	5.00
H(7)	0.072(3)	0.777(11)	0.169(6)	5.00

Table 6. Bond distances (Å) in the salicylato ligands.

Bond	$[Mn(Hsal)_2(H_2O)_2]_2$[a]	$[Mn(Hsal)_2(H_2O)_2]_2$[a]	$[Ni(Hsal)_2(H_2O)_4]$	$[Cu(Hsal)_2(H_2O)_2]\cdot 2H_2O$	$[Zn(Hsal)_2(H_2O)_2]$
C(1)–C(2)	1.398(1)	1.387(1)	1.405(1)	1.392(1)	1.400(5)
C(1)–C(6)	1.383(1)	1.390(1)	1.401(1)	1.389(2)	1.352(10)
C(1)–C(7)	1.474(1)	1.483(1)	1.490(1)	1.485(2)	1.513(10)
C(2)–C(3)	1.390(1)	1.391(1)	1.391(1)	1.382(2)	1.393(10)
C(3)–C(4)	1.342(2)	1.380(1)	1.377(1)	1.369(3)	1.351(9)
C(4)–C(5)	1.387(1)	1.370(1)	1.386(2)	1.375(3)	1.409(9)
C(5)–C(6)	1.381(1)	1.381(1)	1.383(1)	1.384(2)	1.374(9)
C(2)–O(3)	1.344(1)	1.368(1)	1.359(1)	1.359(2)	1.339(9)
C(7)–O(1)	1.267(1)	1.263(1)	1.295(1)	1.264(2)	1.278(7)
C(7)–O(2)	1.264(1)	1.246(1)	1.237(1)	1.260(2)	1.254(6)
H(1)–C(3)	0.78(1)	1.07(1)	1.00(1)	0.96(2)	0.89(5)
H(2)–C(4)	1.07(1)	0.96(1)	0.95(1)	0.93(2)	0.90(5)
H(3)–C(5)	1.01(1)	0.99(1)	0.98(1)	0.95(2)	0.89(5)
H(4)–C(6)	0.95(1)	1.02(1)	1.04(1)	1.14(2)	1.00(5)
H(5)–O(3)	0.70(1)	1.01(1)	0.92(1)	0.98(2)	0.52(6)
H(5)–O(1)	2.02(1)	1.57(1)	1.64(1)	1.66(2)	2.14(5)

[a]There are two asymmetric salicylato ligands in $[Mn(Hsal)_2(H_2O)_2]_2$.

similarly in **1**, **2** and **4** viz. towards the coordinated oxygen atoms O(1) in the carboxyl groups (see Figs. 1, 2, and 4). In **3** the intramolecular hydrogen bonds are formed between the phenol groups and the uncoordinated oxygen atoms O(1) (Fig. 3).

$[Mn(Hsal)_2(H_2O)_2]_2$ is a binuclear complex in which the two manganese atoms are bound together by two bridging salicylato ligands. In addition, both Mn atoms are ligated by one chelating salicylato ligand (Fig. 1). The distance between

Table 7. Bond distances (Å) and angles (°) around metal atoms.

Distance		Angle	
Mn–Mn	3.7140(1)	O(4)–Mn–O(5)	172.58(2)
Mn–O(1)	2.2399(5)	O(1)–Mn–O(2)	56.47(2)
Mn–O(2)	2.3619(5)	O(1)–Mn–O(4)	93.69(2)
Mn–O(4)	2.1509(5)	O(1)–Mn–O(5)	87.32(2)
Mn–O(5)	2.1929(5)	O(1)–Mn–O(11)	137.02(2)
Mn–O(11)	2.2094(5)	O(1)–Mn–O(12)	164.36(2)
Mn–O(12)	2.5647(5)	O(1)–Mn–O(12)′	93.41(2)
Mn–O(12)′	2.1228(5)		
Ni–O(1) (×2)	2.0136(5)	O(1)–Ni–O(4)	90.78(2)
Ni–O(4) (×2)	2.1003(7)	O(1)–Ni–O(5)	88.65(2)
Ni–O(5) (×2)	2.0487(6)	O(4)–Ni–O(5)	89.45(3)
Cu–O(2) (×2)	1.938(1)	O(2)–Cu–O(4)	91.51(5)
Cu–O(4) (×2)	1.914(1)		
Zn–O(1) (×2)	1.982(4)	O(1)–Zn–O(1)′	131.56(16)
Zn–O(4) (×2)	1.998(4)	O(1)–Zn–O(4)	120.93(17)
Zn–O(2) (×2)	2.523(4)		

manganese atoms, symmetry-related by the inversion centre, is 3.714 Å.

In contrast to **1**, complexes **2**–**4** are mononuclear, the salicylato ligands being either monodentate (**2**, **3**) or bidentate (**4**). The coordination polyhedron around the metal atom is different in each structure.

The Mn^{2+} ion (d^5) shows a variety of coordination geometries because the high-spin complexes have no ligand field stabilization energy. Here, manganese has coordination number seven with a pentagonal bipyramidal coordination polyhedron, which is not very common for Mn^{2+} with oxygen-donor ligands. Seven coordination in manganese complexes is normally encountered with macromolecules containing N as donor

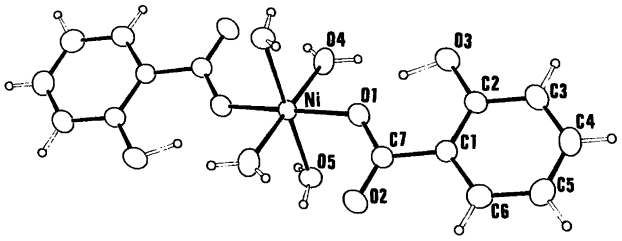

Fig. 2. A perspective view of the $[Ni(Hsal)_2(H_2O)_4]$ molecule (**2**).

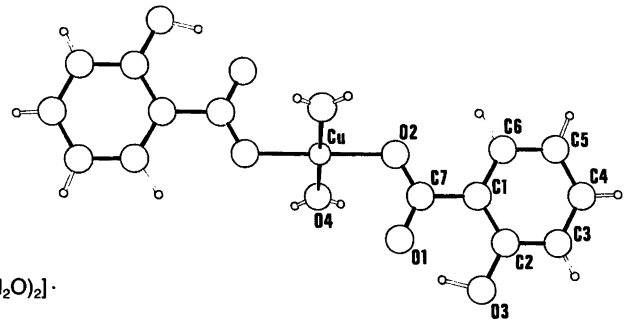

Fig. 3. A perspective view of the $[Cu(Hsal)_2(H_2O)_2] \cdot 2H_2O$ molecule (**3**).

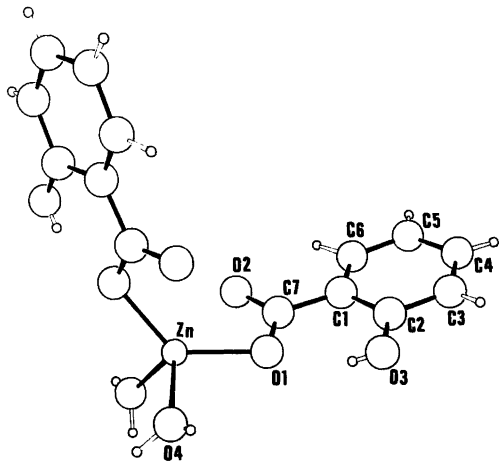

Fig. 4. A perspective view of the $[Zn(Hsal)_2(H_2O)_2]$ molecule (**4**).

atoms.[16] The coordination polyhedron in **1** can be described as pentagonal bipyramidal, where manganese and the oxygen atoms O(1), O(2), O(11), O(11)′ and O(12) form a plane and the oxygen atoms O(4) and O(5) are capping atoms (see Fig. 1 and Table 7).

Co^{2+} and Ni^{2+} have a larger number of *d* electrons than Mn^{2+} and are octahedrally coordinated in salicylato complexes. The octahedron in **2** is very regular (Fig. 2, Table 7) while that around Co^{2+} is distorted, possibly due to the Jahn-Teller effect.[3]

The Cu^{2+} ion (d^9) has coordination number four in **3**. The coordination polyhedron is a square plane as a result of an extreme elongation of two Cu–O distances (> 3.0 Å). The CuO_4 and the salicylato planes form an angle of 117.4°. The coordination of copper is different in the two other known copper salicylato complexes. When the non-coordinated water molecules are absent the polyhedron is a square pyramid.[3] When the non-coordinated water molecules are substituted with dioxane a $[Cu(Hsal)_2(H_2O)_2]_2$ dimer with octahedral coordination around coppper is formed.[17]

The coordination polyhedron around zinc in **4** is ambiguous. There are four short Zn–O distances (ca. 2 Å) involving the water molecules and two oxygen atoms from the carboxyl groups of different salicylato ligands. In addition, there are two longer Zn-O distances (ca. 2.5 Å) involving the remaining oxygen atoms of the carboxyl groups (see Fig. 4 and Table 7). The bidentate salicylato ligands are in *cis* position. The chelating coordination of the COO^- group is also indicated by the IR spectrum of the complex. The polyhedron is unusual for zinc, which normally has quite regular coordination polyhedra with coordination numbers of four or six. Since zinc has a d^{10} electron configuration, ligand field stabilization energy cannot be expected. The stereochemistry including that in the present salicylato complex, will therefore be dominated, by steric factors and electrostatic interactions.

In all the structures the three-dimensional networks are formed via hydrogen bonds. It is interesting to note that all the structures display an intramolecular hydrogen bond in each salicylato ligand involving the hydrogen atom of the phenol group (O3) and one of the carboxyl oxygen atoms (O1).

Infrared spectra. The IR spectra of solid salicylato complexes can be divided in to several regions: 3500–3000 cm^{-1}, the stretching absorptions of the OH-groups origination both from water molecules and from phenol groups, 2000–1650 cm^{-1}, combination vibrations, 1650–1380 cm^{-1}, involving both the C–O stretching of the carboxyl group and aromatic C–C stretching vibrations, 1350–1335 cm^{-1}, the C–O–H bending of the phenol groups, 1260–1230 cm^{-1}, stretching of the phenol groups, 1200–1050 cm^{-1}, bending in the C–H–C plane in the substituted aromatic rings, 880–820 cm^{-1}, scissoring vibrations in the carboxyl groups, 760–740 cm^{-1}, out of plane bending of hydrogen atoms in the benzene rings, and 700–400 cm^{-1}, bending in the benzene rings.

Absorption peaks found in the spectra could be interpreted as follows according to Refs. 8, 9 and 18–20. Most of the peaks in the IR spectra are caused by the planar and regular salicylato ligand in each complex. Therefore, all the spectra are essentially similar and resemble that of the free ligand. The main difference from the spectrum of salicylic acid is that the C–O stretching vibration of the carboxyl group at 1658 cm^{-1} is split in the spectra of the complexes into two peaks which are shifted to lower energies. The maxima of the peaks lie between 1570 and 1540, and 1400 and 1385 cm^{-1}, depending on the complex, indicating the lengthening of the C–O bond. This lengthening is caused by the withdrawal of electron den-

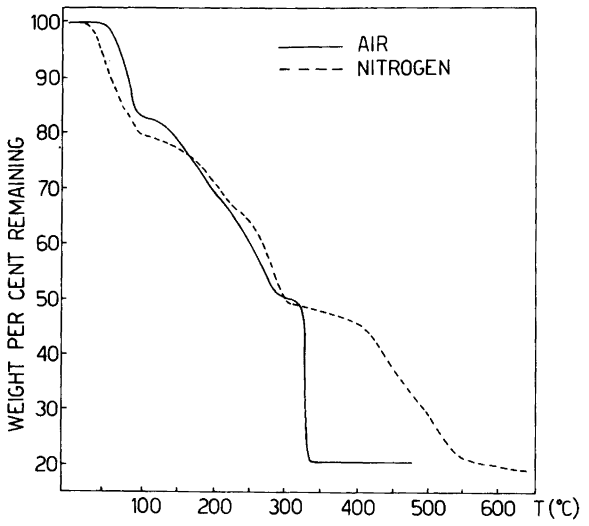

Fig. 5. The TG curves for $[Co(Hsal)_2(H_2O)_4]$ heated in air and in nitrogen.

sity from the ligating carboxyl oxygen atoms towards the metal atom. The two strong peaks at 1570 and 1395 cm^{-1} observed for **2** and **3** indicate the monodentate coordination. In **4** the ligand is bidentate and there is only one intense peak at 1385 cm^{-1} with a small shoulder at 1570 cm^{-1}. In the manganese complex the coordination is different, and there are both bidentate and bridging carboxyl groups. The two C–O stretching vibrations are closer to each other than in the other complexes, viz. at 1540 and 1400 cm^{-1}, and the peaks are slightly broadened.

The IR spectra of the complexes also yielded structural information on the phenol group. In all the complexes **1–4** the OH group in the phenol moiety is free and the C–O–H bending vibrations are detectable. In $[Cu(Hsal)_2(H_2O)_2]$ this mode is absent because of coordination through the phenol group, as shown in the structure.[4] There are two strong deformation vibrations of COO^- at 880–820 cm^{-1} in metal complexes, while in salicylic acid the free group gives rise to only one absorption peak of medium intensity.

Due to the limitations of the instrument used the very interesting far-infrared region, in which the absorptions due to M–O vibrations occur, could not be investigated.

Thermal analyses. The thermal behaviour of **1**, **2**, **4** and $[Co(Hsal)_2(H_2O)_4]$, which is isomorphous with the correponding nickel complex (**2**), is similar. The decomposition of these complexes is exemplified with $[Co(Hsal)_2H_2O)_4]$, as shown in Fig. 5.

In air, the decomposition occurs in three stages: (i) dehydration, (ii) the release of the first salicylato ligand and (iii) the release of the second salicylato ligand combined with the formation of metal oxide. The dehydration is, in all cases, a single step process and occurs at relatively low temperatures (80–150 °). The stability region of the anhydrous phase is limited and the release of H_2sal begins above 120 °C. The weight of the residue remaining after this fast reaction corresponds well to the formula Co(sal). This intermediate phase is unstable. In air, the second salicylato ligand is released between 300 and 330 °C. In the zinc complex (**4**), which is the most stable one, the corresponding reactions take place at considerably higher temperatures.

In nitrogen, the two first decomposition steps are similar to those in air. The stability of the intermediate products is similar in both atmospheres. The release of the second salicylato ligand is, however, slower in nitrogen than in air. The TG curve shows several small steps, the origin of which could not be definitely established.

The difference in the product distribution associated with the release of the first and second salicylato ligands [steps (ii) and (iii)] was studied by mass spectrometry, which indicated two different decomposition mechanisms. Fig. 6 shows that in step (ii) salicylic acid (mass number 138) is evolved which then decomposes to

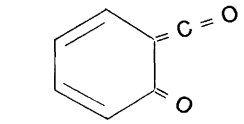

(mass number 120)

and

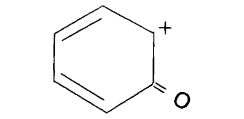

(mass number 92)

releasing water and carbon monoxide simultaneously. In step (iii) salicylic acid, phenol (mass number 94) and carbon monoxide (mass number 44) are evolved. It is possible that the results discussed above are valid only for particular experimental conditions. In air, the release of the second salicylato ligand step (iii) is so fast that the mechanism may be different.

The decomposition pathway for copper complexes, both **3** and $[Cu(Hsal)_2(H_2O)_2]$, cannot be definitely established from the experimental TG data. The intermediate plateau at 250 °C (Fig. 7) does not correspond to the formation of Cu(sal) since the mass of the residue is greater than the theoretical. According to Bassi *et al.*[21] decomposition leads to the formation of $CuCO_3$ and H_2sal. This seems improbable since the sublimation

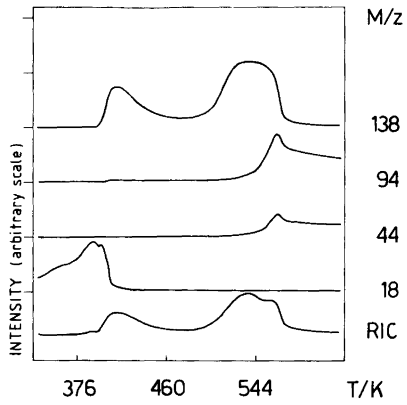

Fig. 6. Ion chromatograms for the heating of $[Zn(Hsal)_2(H_2O)_2]$ (**4**) in a mass spectrometer, showing the mass numbers of different released molecules.

temperature of salicylic acid (172 °C) is much lower than the stability temperature range of the intermediate. The X-ray powder diffraction pattern of the intermediate phase did not contain any lines corresponding to copper (II) carbonate. The intermediate phase may, however, in addition to the carbonate ion also contain some coordinated salicylato ligands. The separate mass spectroscopic studies on the intermediate product

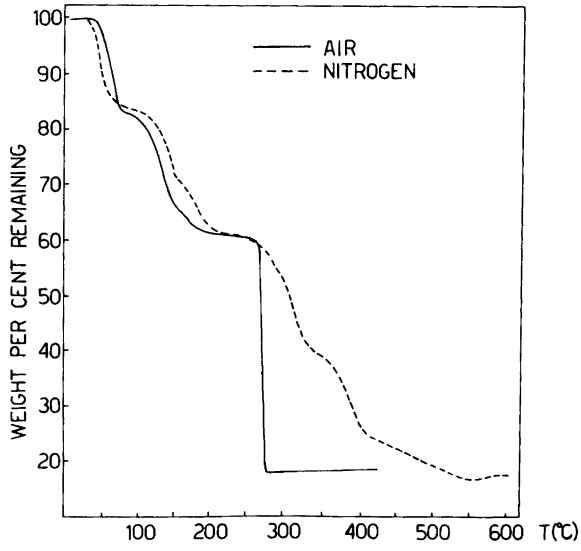

Fig. 7. The TG curves for $[Cu(Hsal)_2(H_2O)_2] \cdot 2H_2O$ (**3**) heated in air and in nitrogen.

indicated that the decomposition products are those observed for **1–4**. No "extra" CO_2 originating from the carbonate ion was detected.

It is interesting to note that the TG curve for a mechanical mixture of $CuCO_3$ and H_2sal showed that they form an intermediate compound of unknown composition upon heating. This compound decomposes similarly to the intermediate phase obtained in the decomposition of salicylato complexes **3** and $[Cu(Hsal)_2(H_2O)_2]$.

Acknowledgement. Dr. R. Laitinen (Helsinki University of Technology) is gratefully acknowledged for valuable discussions.

References

1. Hanic, F. and Michalov, J. *Acta Crystallogr. 13* (1960) 299.
2. Jagner, S., Hazell, R. G. and Larsen, K. P. *Acta Crystallogr., Sect. B 32* (1976) 548.
3. Klug, H. P., Alexander, L. E. and Summer, G. G. *Acta Crystallogr. 11* (1958) 41.
4. Gupta, M. P. and Mahanta, B. *Cryst. Struct. Commun. 7* (1978) 175.
5. Gupta, M. P. and Ashok, *J. Curr. Sci. 47* (1978) 534.
6. Mishra, H. G. and Jha, R. R. *J. Indian Chem. Soc. 56* (1979) 525.
7. Bassi, P. S., Kalsi, P. C. and Kharuija, C. M. *Thermochim. Acta 34* (1979) 183.
8. Heda, B. D. and Khadikar, P. V. *Bull. Soc. Chim. Belg. 89* (1980) 1.
9. Kishore, K. and Nagarajan, R. *J. Therm. Anal. 22* (1981) 25.
10. Lajunen, L. H. J. and Kokkonen, P. *Thermochim. Acta 85* (1985) 55 and references therein.
11. Cromer, D. T. and Mann, J. B. *Acta Crystallogr., Sect. A 24* (1968) 321.
12. Gilmore, C. J. *J. Appl. Crystallogr. 17* (1984) 42.
13. Stewart, J. M. *The X-Ray 76 System.* Technical Report TR-446, Computer Science Center, University of Maryland, College Park, MD 1976.
14. Johnson, C. K. *ORTEP II: A Fortran Thermal Ellipsoid Plot Program for Crystal Structure Illustrations,* Oak Ridge National Laboratory, Oak Ridge, TN 1976.
15. Lajunen, L. H. J., Kokkonen, P., Nissi, A. and Ruotsalainen, H. *Thermochim. Acta 72* (1984) 219.
16. Drew, M. G. B., Hamid, O. A., McFall, S. S., McIlroy, P. D. A. and Nelson, S. M. *J. Chem. Soc., Dalton Trans.* (1977) 438.
17. Ablov. A. V., Kiosse, G. A., Dimitrova, G. I., Malinovski, T. I. and Popovich, G. A. *Kristallografiya 19* (1974) 168.
18. Babko, A. K. and Shevchenko, L. L. *Russ. J. Inorg. Chem. 9* (1964) 22.
19. Kharitonov, Y. Y. and Tuiebakhova, Z. K. *Koord. Khim. 9* (1983) 1512.
20. Kharitonov, Y. Y. and Tuiebakhova, Z. K. *Russ. J. Inorg. Chem. 29* (1984) 811.
21. Bassi, P. S., Kalsi, P. C. and Khajuria, C. M. *Indian J. Chem., Sect. A 15* (1977) 399.

Received January 30, 1987.